Numerical modelling of tunnel liner and fracture interaction

by D.F. Malan* and J.A.L. Napier

Synopsis

Considerable practical knowledge and effective use of empirical evidence is required in the design of tunnel support systems. In many instances, it is unclear how individual support elements interact with fractured rock and which elements of the support system are critical in controlling and containing the movement of material proximate to the excavation. The present paper outlines a displacement discontinuity approach that allows the coupling of surface constraints, in the form of liner or mesh material, to an explicit representation of time-dependent rock discontinuity creep movements. The method is illustrated for a simple square-shaped tunnel profile in which the fracture zone is mobilized by an imposed stress field. A crucial aspect of the model is the computational treatment of the coupling between the liner material and the representation of the fractured rock mass. This allows the response of the liner material to be assessed quantitatively in terms of the possible reduction of movement in the rock mass. The importance of installing the liner timeously after the excavation is formed is illustrated in a specific example. A number of computational difficulties in simulating liner-rock interaction mechanisms are identified.

Introduction

The use of liners in tunnel excavations in soft ground or at great depths is essential to ensure the stability and safety of these structures. Historical aspects of liner usage in tunnel design have been reviewed by Kovari (2003). In the case of deep-level mine tunnel excavations, design procedures have to acknowledge the transient nature of mining activity and excavation safety has to be ensured, in principle, only for as long as mining operations are continued. The design of such excavations, where multiple support strategies may be deployed, is necessarily often based primarily on empirical experience and on site-specific adaptations to local geotechnical conditions. The exact mechanisms of multiple support structure interactions are extremely complex. In addition, loading conditions are imprecisely quantified in mining environments where the extension of nearby excavations may enhance, decrease or rotate the principal stress load state at a given location, over a period of time.

Computational modelling of these situations is becoming increasingly prominent and ranges, for example, from analysis of bolt lengths (Goel *et al.*, 2007) to parametric studies of the behaviour of simple liner-rock models (Stacey and Yu, 2004). More challenging applications have addressed the problem of replicating observed seismic activity near excavations (Cai *et al.*, 2007) and recently the simulation of fragmentation and dynamic failure under extreme loading rates (Morris *et al.*, 2006, Heuze and Morris, 2007). An important practical aspect of mine tunnel performance is, less dramatically, the ongoing creep-like deformation of the rock mass or 'squeezing' after the formation of the tunnel (Barla, 1995). When a tunnel is driven into soft squeezing rock (such as soft clays or mudstone), the ground advances slowly into the opening without visible fracturing or loss of continuity (e.g. Gioda and Cividini, 1996). Squeezing can, however, also involve different mechanisms of discontinuous failure of the surrounding rock. Possible mechanisms are complete shear failure in rock if the existing discontinuities are widely spaced, buckling failure in thinly bedded sedimentary rocks and sliding failure along bedding planes (Aydan *et al.*1996). Figure 1 illustrates squeezing conditions in hard rock at Hartebeestfontein Gold Mine in South Africa where the mechanism of squeezing is a combination of sliding along low-friction bedding planes and time-dependent fracture processes.

* *Groundwork Consulting (Pty), Johannesburg.*

† *CSIR Pretoria and School of Computational and Applied Mathematics, University of the Witwatersrand, Johannesburg.*

Numerical modelling of tunnel liner and fracture interaction

Figure 1—Haulage conditions experienced in the squeezing rock at Hartebeestfontein Mine (courtesy W.D. Ortlepp)

Haile (1996) described a support strategy that appeared to be successful in a squeezing tunnel at Kloof Gold Mine. The tunnel was developed at a depth of approximately 3 000 m in rock characterized by a high frequency of bedding planes with infilling, which resulted in a low rock mass strength. The support strategy consisted of the immediate application of a 25 mm shotcrete layer and primary bolting as close as possible to the development face. Approximately 15 m behind this face, additional support was installed consisting of a 75 mm steel fibre-reinforced shotcrete layer, secondary bolting and wiremesh and lacing. This appeared successful in controlling the deformation. This particular strategy highlights the importance of timing of support installation in potential squeezing conditions. If too much time elapses before the installation of support, the rock may undergo unravelling, making it more difficult to control (Steiner, 1996). Pan and Dong (1991) and Pan and Huang (1994) analysed the effect of time of support installation in squeezing rock by assuming that the rock behaves in a viscoelastic fashion. Results indicate that earlier support installation ensures a lower tunnel convergence. This is, however, accompanied by higher support pressures (Cristescu *et al.*, 1987; Sakurai, 1978), which may lead to rapid failure of the support in heavy squeezing rock. In summary, it appears that the rock time response needs to be matched to the ability of the liner material to reach full resistive capacity following its installation. In the case of thin sprayed liners, the fully cured strength of the liner material is achieved only some time after the installation of the liner. In certain instances this time may vary from two to four weeks (Yilmaz, 2007). More fundamentally, it is also not very clear exactly how such a spray-on liner material is loaded when adjacent blocks in the tunnel walls slip relative to the restraining liner-rock interface. The present paper attempts to highlight some of the basic mechanisms that may arise and the corresponding response of the liner material.

Simulation model

The displacement discontinuity boundary element method (Crouch and Starfield, 1983) is used in the present study to simulate the interaction of multiple crack segments in the rock mass near an excavation. Multiple material zones are treated by specifying superimposed pairs of displacement discontinuity elements on each bi-material interface in the model. In these cases the discontinuity density in both elements is determined by simultaneously solving for appropriate displacement and traction boundary conditions at the interface element collocation points. Remote influence transmissions are computed from elements belonging to the respective individual zones corresponding to each member of the interface element pair. Displacement discontinuity slip and opening shape functions can be chosen to have linear, quadratic or cubic variations along the length of each element, satisfying 'collocated' boundary conditions at two, three or four specified points within each element. In addition, time-dependent creep effects are simulated by postulating that the discontinuity slip rate at each element collocation point is proportional to the difference between the local shear stress, and the shear resistance, at that point. In particular, it is assumed that

$$dD_s / dt = \kappa(\tau - \rho), \qquad [1]$$

where Ds is the extent of slip, t is the time and κ is a proportionality constant ('fluidity'). In this relationship, the shear resistance, ρ, is assumed to be the sum of a friction resistance term and a cohesion term. The cohesion is allowed to be a function of the extent of slip (slip-weakening behaviour).

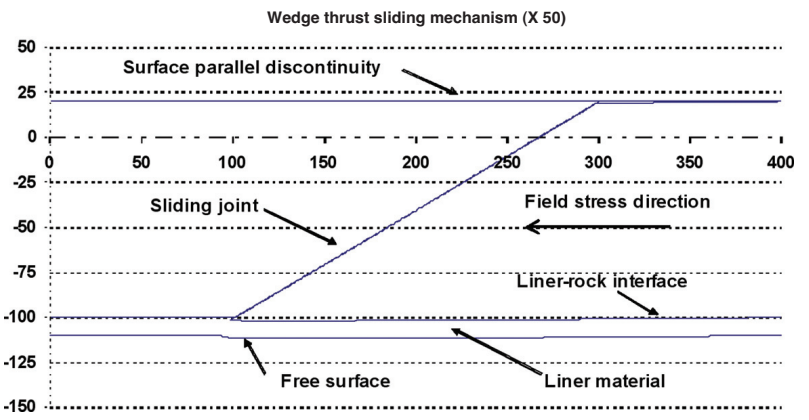

Figure 2—Simple mechanism of the interaction of a bonded liner material with a sliding wedge

Simple wedge deformation mechanisms

In order to gain some perspective of the interaction of a liner layer with an adjacent sliding discontinuity, consider the simple case illustrated in Figure 2. In this instance, a discontinuity in the rock mass of nominal length equal to 400 mm is assumed to be parallel to a local excavation surface and is intersected by an inclined sliding joint that also intersects the free surface (see Figure 2). It is assumed that an elastic layer having a nominal thickness of 10 mm is bonded to the rock surface and restrains the joint sliding movement when a far field load is applied parallel to the excavation surface. The magnified joint deformation displacement (magnification factor 50) resulting from a surface-parallel load of 100 MPa is shown in Figure 2. The rock mass modulus is assumed to be equal to 7 0000 MPa and the liner material is assumed, in this case, to be elastic and to have a modulus of 1 000 MPa. The Poisson's ratio is set to 0.2 in both cases. Although the slip movements indicated in Figure 2 are small (of the order of 1 mm), it is observed that the shear and normal stress components arising near the liner-rock interface can be extremely large, as shown in Figure 3. Figure 3 also illustrates the effect of increasing the liner material modulus from 1 000 MPa to 7 000 MPa and indicates that the interface stress magnitudes are correspondingly magnified.

The actual slip distribution along the sliding joint is shown in Figure 4. It is apparent that the bonded liner reduces the slip extent although the degree of this reduction is interestingly not as dramatic as might be expected from the extreme nature of the imposed constraint (i.e. the perfect bonding of the liner to the excavation surface). The shapes of the slip profiles in Figure 4, with the liner in place, also indicates that close to the joint-liner intersection point (distance = 0 in Figure 4) the stress magnitudes in the liner will be singular as shown in Figure 3. This suggests that in practice, such a liner would be expected to experience 'plastic' deformation or to debond in the vicinity of the joint intersection point. The behaviour at joint-surface intersection points is therefore most crucial in assessing the overall ability of the liner material to contain near-surface rock mass movements. The validity of assuming a perfectly elastic, bonded liner material also becomes highly questionable.

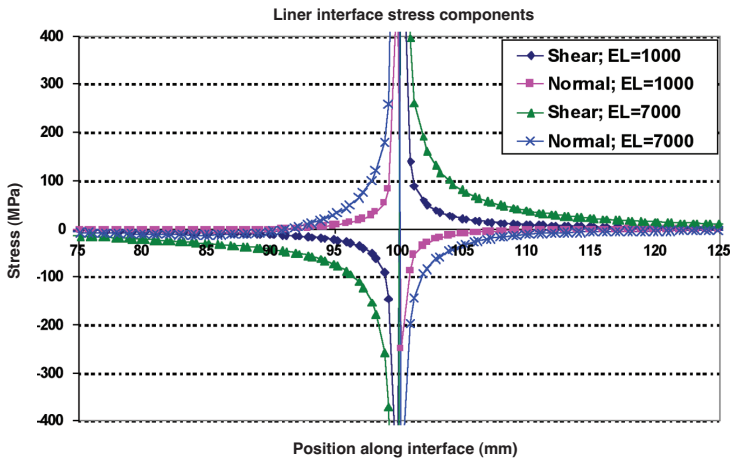

Figure 3—Shear and normal stress components for the rock-liner interface for modulus values of 1 000 MPa and 7 000 MPa applied to the simulated liner material

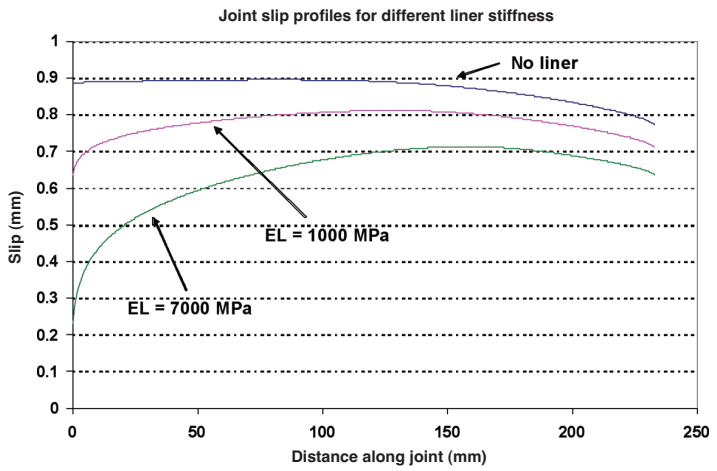

Figure 4—Distribution of slip magnitude along the inclined joint depicted in Figure 1 for the cases of liner modulus (EL) equal to 1 000 MPa and 7 000 MPa respectively and for the case where no liner is present

A simplified model of liner behaviour

In the absence of detailed inelastic constitutive descriptions for specific liner materials, a simplified modelling approach is assumed in this paper. Specifically, it is postulated that the sliding and opening behaviour of the joint itself can be suitably amended close to the excavation surface, where the liner is attached, to provide equivalent deformation constraints to the case of a multiple zone model that includes the liner material explicitly. In the displacement discontinuity model adopted here, this is most conveniently achieved by introducing a special 'constitutive law' at the joint element collocation point that is immediately adjacent to the excavation surface. This scheme is illustrated in Figure 5 for the case of quadratic variation displacement discontinuity elements having three internal collocation points. Although this approach may appear to be overly simplistic, consider the simplest case where no shear or opening of the discontinuity is allowed at the edge point. Figure 6 illustrates the corresponding joint slip profile (marked as 'pinned') and it can be observed that this is remarkably similar to the slip profile shown in Figure 4 corresponding to the liner having a Young's modulus of 7 000 MPa. Adopting this approach also allows additional models to be developed. For example, it may be assumed that the edge collocation point sliding movement is resisted by a linear spring stiffness modulus, K. The two joint slip profiles shown in Figure 6 correspond to the specific cases where K = 1 0000 MPa/m and K = 20 000 MPa/m respectively. In these cases, it is apparent that the joint movement is not completely arrested at the excavation surface. Further models including, for example, a peak shear yield stress may be accommodated easily as a simple means of representing liner plasticity. The simulation of a bending moment constraint imposed by a very stiff surface lining may also be included by considering the slope of the opening mode displacement discontinuity component at the special edge point. This quantity is related to the relative rotation of the material regions on each side of the joint. These possibilities are not elaborated further in this paper. It should be noted that the edge-collocation model described here may need further elaboration to describe the behaviour of liner material that is deemed to penetrate some distance into surface joints. In particular, the penetration distance would need to be specified and suitable amendments made to all joint element collocation points contained within this distance.

Simulation of time-dependent deformation near a square tunnel

In order to illustrate the behaviour of the proposed liner model, consider the time-dependent deformation of a square tunnel subjected to a remote stress field of 50 MPa in the vertical direction (designated as *Pzz*) and 12.5 MPa in the horizontal direction (designated as *Pyy*). The tunnel side dimension is assumed to be 3 m and the rock mass material properties are summarized in Table I. Rock failure in the region surrounding the tunnel is assumed to occur on the

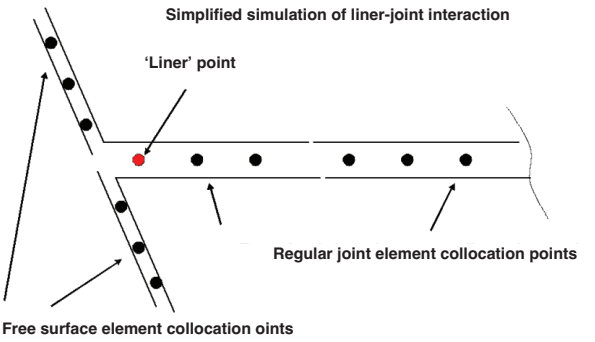

Figure 5—Illustration of simplified modelling strategy to simulate liner behaviour in a displacement discontinuity model of a joint intersecting an excavation surface

Table I
Rock mass properties

Property	Value
Shear modulus	25 000 MPa
Poisson's ratio	0.2
Intact cohesion	5.0 MPa
Intact and residual friction angle	30 degrees
Tensile strength	1.0 MPa
Cohesion slip weakening slope	25 000 MPa/m
Slip 'fluidity' parameter,	0.00001 m/(time*MPa)

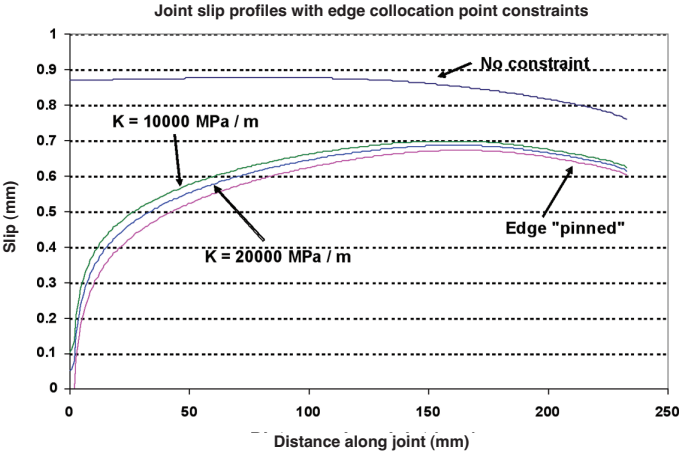

Figure 6—Joint slip profiles simulated by assuming specific slip-opening constitutive rules for the simplified edge collocation point strategy shown in Figure 4

elements of a random Delaunay mesh of discontinuity elements. The rate of slip movement on each mobilized collocation point is updated in a series of time steps by application of Equation [1]. The stress state and the population of mobilized discontinuity elements is updated incrementally during each simulated time step. The Delaunay mesh comprises 3 652 elements having an average length of 0.175 m and is assumed to cover a 10 m by 6 m rectangular region surrounding the tunnel. The extent of the mobilized fracture zone arising after 50 time steps is shown in Figure 7 for the case where no liner is installed on the tunnel surface. The corresponding case where a 'perfect' liner is imposed at the tunnel surface, immediately after the tunnel is formed, is shown in Figure 8. The differences between the two cases are rather small.

A more revealing interpretation of the evolution of the fracture zone is obtained by computing the net energy release increments arising during each simulated time step. The energy release increments for the cases where no liner is installed are compared to the energy release increments with the 'perfect' liner in Figure 9. The corresponding cumulative energy release values for the first 30 time steps are plotted in Figure 10. This indicates that the liner material does inhibit the overall energy release. More importantly, it can be observed from Figures 9 and 10 that the energy release increments decay substantially after 20 time units have elapsed. This emphasizes that the main benefit of installing the liner material can be substantially lost if the liner is not installed soon after the formation of the excavation or if the fully cured strength of the liner material is longer than the characteristic relaxation time of the mobilized rock mass.

It should be noted that the iterative solution of the interactive crack assembly matrix in these cases is prone to being ill conditioned. Special strategies have been implemented to identify and to 'freeze' particular elements in the mobilized crack population in order to improve the iterative performance. This issue warrants further attention.

Conclusions

Computational modelling of the liner-rock interaction is becoming increasingly important to optimize the design of the liners and to gain an improved understanding of the

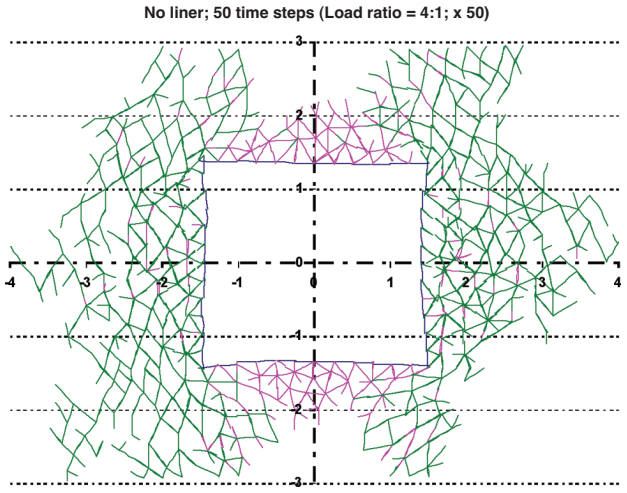

Figure 7—Mobilized pattern of discontinuities after 50 time relaxation steps near a square tunnel without lining and where the far-field vertical stress is 50 MPa and the horizontal stress is 12.5 MPa

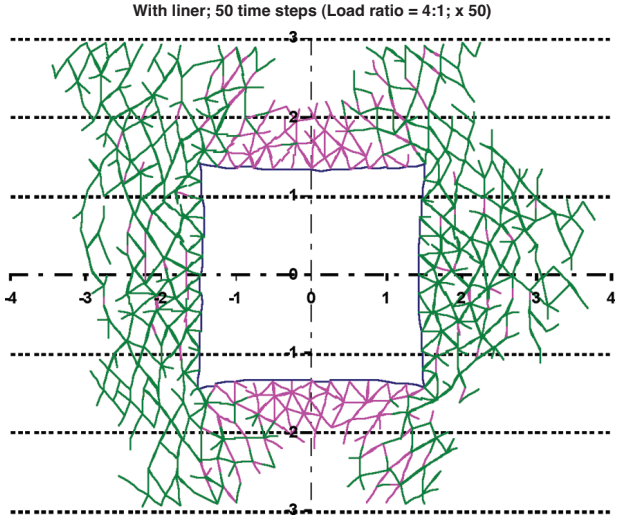

Figure 8—Mobilized pattern of discontinuities after 50 time relaxation steps near a square tunnel with a 'perfect' lining applied to the tunnel surfaces and where the far-field vertical stress is 50 MPa and the horizontal stress is 12.5 MPa

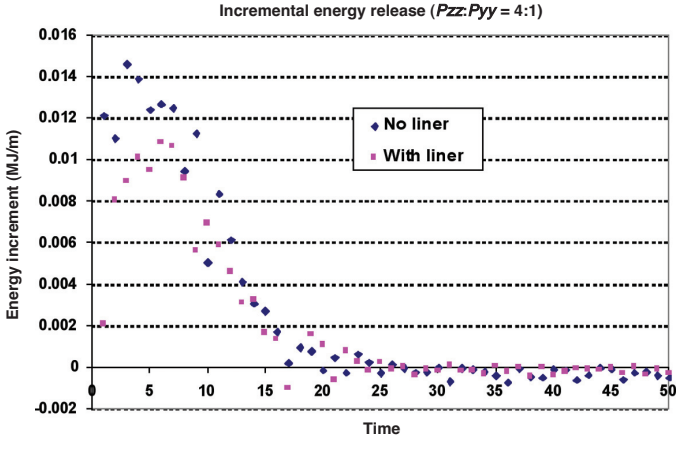

Figure 9—Comparison of energy release increments for rock mass mobilization around a square tunnel with no installed liner and with a 'perfect' liner material that is simulated by fixing the movements on all collocation points of slip segments immediately adjacent to the tunnel surface

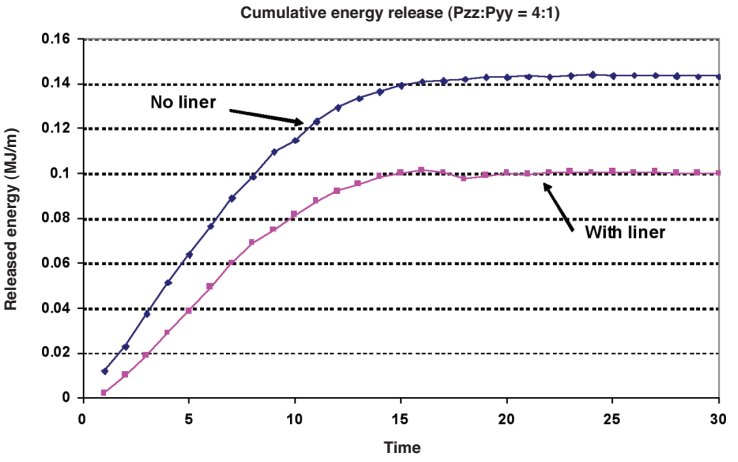

Figure 10—Comparison of cumulative time-dependent energy release for rock mass mobilization around a square tunnel with no installed liner and with a 'perfect' liner material

behaviour of fractured rock when confined by these liners. The present paper outlines a displacement discontinuity approach that allows the coupling of surface constraints, in the form of liner or mesh material, to an explicit representation of time-dependent rock discontinuity creep movements. This model appears to offer some encouraging possibilities for identifying and understanding some of the interaction mechanisms that may arise between liner material and general time-dependent rock mass creep movements. The advantage of the approach is that the creep of prominent discontinuities, such as multiple bedding planes, is easily incorporated. The method is illustrated for the case of a simple square-shaped tunnel profile in which the fracture zone is mobilized by an imposed stress field. A crucial aspect of the model is the computational treatment of the coupling between the liner material and the representation of the fractured rock mass. This allows the response of the liner material to be assessed quantitatively in terms of the possible reduction of movement in the rock mass. The importance of installing the liner timeously after the excavation is formed is illustrated in a specific example. The results emphasize that the main benefit of installing the liner material can be substantially lost if the liner is not installed soon after the formation of the excavation or if the fully cured strength of the liner material is longer than the characteristic relaxation time of the mobilized rock mass.

References

Aydan, Ö., Akagi, T., and Kawamoto, T. The squeezing potential of rock around tunnels: Theory and prediction with examples taken from Japan. *Rock Mech. Rock Engng*. vol. 29, 1996, pp. 125–143.

Barla, G. Squeezing rocks in tunnels. *ISRM News Journal*. vol. 2, no. 3 and 4, 1995, pp. 44–49.

Cai, M., Kaiser, P.K., Morioka, H., Minami, M., Maejima, T., Tasaka, Y., and Kurose, H. FLAC/PFC coupled numerical simulation of AE in large-scale underground excavations. *Int. J. Rock Mech.& Min. Sci*., vol. 44, 2007. pp. 550–564.

Cristescu, N., Fota, D., and Medves, E. Tunnel support analysis incorporating rock creep. *Int. J. Rock Mech. Min. Sci*., vol. 24, 1987, pp. 321–330.

Crouch, S.L. and Starfield, A.M. *Boundary Element Methods in Solid Mechanics*. George Allen & Unwin, London, 1983.

Goel, R.K., Swarup, Anil, and Sheorey, P.R. Bolt length requirement in underground openings. *Int. J. Rock Mech.& Min. Sci*., vol. 44, 2007. pp. 802–811.

Gioda, G. and Cividini, A. Numerical methods for the analysis of tunnel performance in squeezing rocks. *Rock Mech. Rock Engng*., vol. 29, 1996, pp. 171–193.

Haile, A.T. Personal Communication, 1998.

Heuze, F.E. and Morris, J.P. Insights into ground shock in jointed rocks and the response of structures there-in. *Int. J. Rock Mech.& Min. Sci*., vol. 44, 2007. pp. 647–676.

Kovari, K. History of the sprayed concrete lining method—part I: milestones up to the 1960s. *Tunnelling and Underground Space Technology*, vol. 18, 2003. pp. 57–69.

Kovari, K. History of the sprayed concrete lining method—part II: milestones up to the 1960s. *Tunnelling and Underground Space Technology*, vol. 18, 2003. pp. 71–83.

Morris, J.P., Rubin, M.B., Block, G.I., and Bonner, M.P. Simulations of fracture and fragmentation of geologic materials using combined FEM/DEM analysis. *Int. J. Impact Engineering*, vol. 33, 2006. pp. 463–473.

Pan, Y.W. and Dong, J.J. Time-dependent tunnel convergence—II. Advance rate and tunnel-support interaction. *Int. J. Rock Mech. Min. Sci.*, vol. 28, 1991, pp. 477–488.

Pan, Y.W. and Huang, Z.L. A model of the time-dependent interaction between rock and shotcrete support in a tunnel. *Int. J. Rock Mech. Min. Sci*., vol. 31, 1994, pp. 213–219.

Sakurai, S. Approximate time-dependent analysis of tunnel support structure considering progress of tunnel face. *Int. J. Num. Anal. Meth. Geomech*. vol. 2, 1978, pp. 159-175.

Stacey, T.R. and Yu, X. Investigations into mechanisms of rock support provided by sprayed liners. *Ground Support in Mining and Underground Construction*, Villaescusa and Potvin (eds.), Taylor and Francis Group, London, 2004. pp. 565–569.

Steiner, W. Tunneling in squeezing rocks: case histories. *Rock Mech. Rock Engng*. vol. 29, 1996, pp. 211–246.

Yilmaz, H. Shear-bond strength testing of thin spray-on liners. *J. S. Afr. Inst. Min. Metall*., vol. 107, no. 8, 2007. pp. 519–530. ◆